


Article

Evaluation of Some State-Of-The-Art Wind Technologies in the Nearshore of the Black Sea

Florin Onea  and Liliana Rusu * 

Department of Mechanical Engineering, Faculty of Engineering, Dunarea de Jos University of Galati, 47 Domneasca Street, 800008 Galati, Romania; florin.onea@ugal.ro

* Correspondence: lrusu@ugal.ro; Tel.: +40-745-399-426

Received: 25 August 2018; Accepted: 12 September 2018; Published: 15 September 2018



Abstract: The main objective of this work was to evaluate the nearshore wind resources in the Black Sea area by using a high resolution wind database (ERA-Interim). A subsequent objective was to estimate what type of wind turbines and wind farm configurations would be more suitable for this coastal environment. A more comprehensive picture of these resources was provided by including some satellite measurements, which were also used to assess the wind conditions in the vicinity of some already operating European wind projects. Based on the results of the present work, it seems that the Crimea Peninsula has the best wind resources. However, considering the current geopolitical situation, it seems that the sites on the western part of this basin (Romania and Bulgaria) would represent more viable locations for developing offshore wind projects. Since there are currently no operational wind projects in this marine area, some possible configurations for the future wind farms are proposed.

Keywords: Black Sea; wind power; nearshore; reanalysis data; satellite measurements

1. Introduction

The energy market and carbon emissions seem to have a strong connection, and since the energy demand is expected to increase in the near future, the negative impacts on the environments will be more noticeable [1,2]. A possible way to tackle this issue is to use natural resources (such as solar or geothermal) to secure a sustainable future and limit the effects of fossil fuels products [3–5]. One of the most successful sectors is wind energy, which has already demonstrated its technical-economic viability in various parts of the world, being possible to develop projects on land or in the marine environment [6–8]. Coastal areas seem to present much higher wind resources than onshore, while the wind turbulences reported in these regions seem to have a lower impact on turbine performance. Furthermore, the diurnal/nocturnal variations of the air masses in the nearshore areas may increase the performance of a wind generator [9].

By looking at the global offshore wind market (at the end of 2017), we can notice that European countries dominate this sector, as in the case of UK (6.8 GW), Germany (5.3 GW), Denmark (1.2 GW), Netherlands (1.1 GW) or Belgium (0.8 GW). PR China (with 2.8 GW) can be also considered in the front line of this industry, while in the second line we may include countries such as Vietnam, Japan, South Korea, USA or Taiwan, which nevertheless report a cumulated value below 0.5 GW [10]. In 2017, Europe upgraded its offshore parks with almost 560 new turbines, including the first floating project and, on average, the water depth for these projects was around 28 m with a distance to the coastline of 41 km. It is expected that by 2020 the installed capacity will be around 25 GW, which can be achieved if we consider that the average turbine capacity is around 6 MW (+23% reported to 2016) and the average size of a farm is estimated close to 493 MW (+34% compared to 2016) [11].

Offshore wind farms operating in the areas located between 30° and 60° latitude (both hemispheres) are expected to have the best performances, considering the action of the prevailing western winds [12,13]. However, the enclosed basins located in those regions have particular wind conditions, as in the case of the Black Sea environment. Thus, the characteristics of the wind conditions in the Black Sea seem to present interest for the scientific communities, as we can see from the previous works focused on meteorological studies, accuracy assessment of various wave models or renewable studies. Rusu et al. [14,15] assessed the performance of a wind-wave modeling system, where among others the wind resources were evaluated by considering in-situ measurements (reported at 10 m height). According to these works, we may expect average wind speeds around 7 m/s and 6 m/s, in the vicinity of Romanian offshore and nearshore area, respectively. Close to the Crimean Peninsula, an average wind speed of about 5.5 m/s was considered to be representative. Valchev et al. [16] evaluated the storm events from the western part of this region, highlighting that, during such an event, extreme values of the wind speed may be encountered, in the range of 21.8–27.8 m/s. Onea and Rusu [17] evaluated the regional wind potential for an interval of 14 years considering various sources of data, such as reanalysis wind models, satellite measurements and data coming from 11 in-situ stations, which are located close to the Romanian and Ukrainian coastal areas. According to these results, the western part of the sea seems to have more consistent wind resources suitable for a wind project. Akpinar and Ponce de Leon [18] considered several reanalysis wind datasets to model the storm occurrences in the Black Sea. They assessed the accuracy of the numerical simulations by comparing them against real measurements. The potential of the offshore wind resources from the Mediterranean and Black Sea were assessed by Koletsis et al. [19] considering the climatological changes. This list can continue, mentioning at the same time the DAMWAVE [20] and ACCWA [21] projects which involve wind data reported on long term.

Regarding the renewable studies involving offshore wind turbines, we can mention that there are fewer studies focused on this region, and probably related to the fact that the Black Sea area is considered less attractive for such projects. Davy et al. [22] briefly discussed the performance of Enercon E-126 wind turbine (7.6 MW) for the Black and Azov Seas, while Onea and Rusu [23] discussed the expected efficiency of a Siemens 2.3 generator which may operate in the northwestern part of this basin. Ilkilic and Aydin [24], in a review study, provided a complete description of wind projects that operate in the Turkish coastal regions (onshore). The expected energy performances of some commercial offshore wind turbines were assessed by Onea and Rusu [25] for several sites distributed along the Black Sea coastline at a water depth of about 50 m. According to these results, during the nocturnal interval, the wind turbines considered may have better performance than in the diurnal period. Argin and Yerci [26] proposed several offshore sites that seem to be suitable for the development of a wind project. Raileanu et al. [27] focused on the performance assessment of two offshore wind turbines (Siemens SWT-3.6-120 and Senvion 6.2M 126) by using satellite measurements recorded between January 2010 and December 2014.

In this context, the objectives of the present work were: (1) to assess the Black Sea wind characteristics by using a reanalysis product defined by a relatively high resolution ($0.125^\circ \times 0.125^\circ$); (2) to estimate the performances of several state-of-the-art wind turbines, including a generator rated at 9.5 MW; and (3) to identify the configurations for wind projects that are suitable for the Black Sea coastal areas.

2. Materials and Methods

2.1. The Target Area

The Black Sea is a semi-enclosed basin defined by an area of 423,000 km² and a maximum depth of 2258 m. The geographical coordinates of its extreme points are 41°N/46°N and 27°E/42°E. In the western part, an extended continental shelf defined by a lower water level can be noticed, while for the rest of the sea a steep continental slope ends with a flat sea bed, where the depths easily exceed

2000 m. On a large scale, the wind conditions are under the influence of the Siberian and Azores high-pressure areas and by the Asian low-pressure area. It is expected that during the wintertime, the prevailing wind speeds (predominant values) are around 8 m/s (from northeast), while during the summer time we may expect wind conditions of 2–5 m/s coming from the northwest [28]. In addition, it is important to mention the local winds such as the breezes, which can account for 190 days/year in the southern part of Crimea, while this event is less noticeable in the western part of the sea. Since this area is surrounded by mountains, it is possible to notice some local events, such as the Bora wind which is more visible in the vicinity of the Novorossiysk region, being caused by the strong northeast Arctic wind collapsing through Kolkhida Lowland [17,29].

Figure 1 illustrates the locations of the twenty reference sites (denoted clockwise from P1 to P20) considered for assessment, which are distributed between four sectors (A–D). Each site is associated to a major Black Sea city or harbor, as shown in Table 1. Furthermore, they were defined in water depths of 26–31 m, being the average depth at which we may find most European wind projects [11]. However, the sites Odessa (14 m) and Kerch (11 m) have smaller depths, while the last one is located in the Azov Sea. A maximum distance from the shore of 42 km corresponds to Site P3 (Bilhorod-Dnistrovskiy, Ukraine), while a minimum of 0.9 km is indicated for Site P19 (Primorsko, Bulgaria).

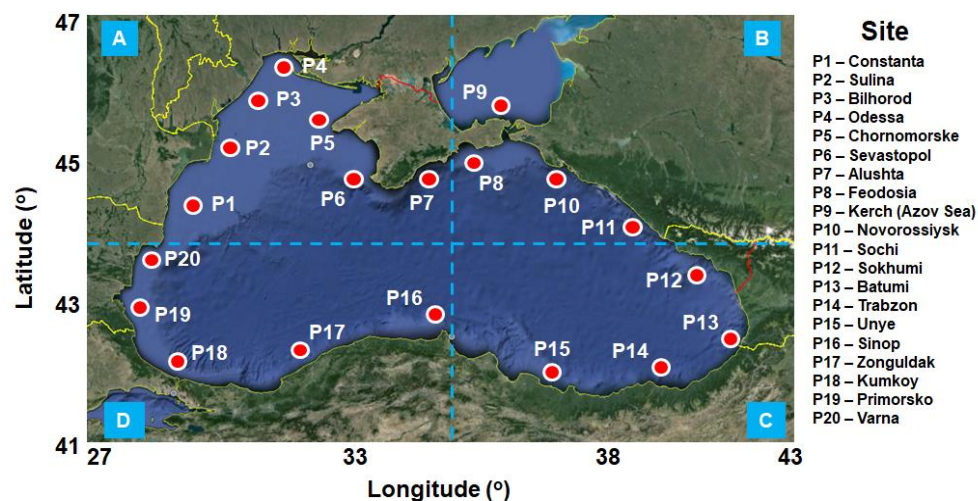


Figure 1. The Black Sea area and the location of the reference sites (map from Google Earth, 2018).

Table 1. The main characteristics of the sites considered.

No.	Site	Country	Sector	Long (°)	Lat (°)	Water Depth (m)	Distance from Coastline (km)
P1	Constanta	Romania	A	28.77	44.15	31	9.32
P2	Sulina		A	29.90	45.09	28	7.17
P3	Bilhorod-Dnistrovskiy	Ukraine	A	30.82	45.78	26	42.37
P4	Odessa		A	31.18	46.45	14	32
P5	Chornomorske	Russia	A	32.66	45.57	28	6.93
P6	Sevastopol		A	33.36	44.58	32	1.46
P7	Alushta		A	34.45	44.66	30	3.16
P8	Feodosia		B	35.52	44.95	30	9.66
P9	Kerch (*Azov Sea)		B	36.48	45.61	11	18.11
P10	Novorossiysk		B	37.77	44.62	31	3.23
P11	Sochi		B	39.68	43.57	30	1.95
P12	Sokhumi		C	41.02	42.97	29	3.19
P13	Batumi	Georgia	C	41.56	41.64	31	3.59
P14	Trabzon	Turkey	C	39.71	41.02	32	1.4
P15	Unye		C	37.31	41.15	33	3.44
P16	Sinop		D	35.14	42.04	30	2.09
P17	Zonguldak		D	31.76	41.47	31	2.54
P18	Kumkoy		D	29.04	41.27	28	2.14
P19	Primorsko	Bulgaria	D	27.77	42.26	30	0.87
P20	Varna		D	28.21	43.13	30	22.34

2.2. Dataset

The reanalysis wind data considered in the present work are provided by the European Centre for Medium-Range Weather Forecasts (ECMWF) [30,31]. Thus, the considered ERA-Interim product is defined by a high spatial resolution of $0.125^\circ \times 0.125^\circ$, a temporal resolution of 6 h (associated to 00:00–06:00–12:00–18:00 UTC) and a 20-year time interval from January 1998 to December 2017. The wind fields are reported to a 10 m height above the sea level, and in this case the wind speed is denoted with U_{10} (m/s). For large water areas, the ERA-Interim data are frequently used to assess the wind potential on various regions, such as Global [32,33], Europe [34–36], South China Sea [37], South Korea [38] or Chile [39]. Another dataset used in this work comes from the AVISO (Archiving, Validation and Interpretation of Satellite Oceanographic Data) project, and includes gridded near-real time wind speeds. This is a multi-mission product, which means that data from at least two missions, such as TOPEX/Poseidon, OSTM/Jason-2 or Saral/AltiKa, need to be available [40,41]. The NetCDF files provided by AVISO include measurements of the U_{10} parameter, which are available for the time interval from September 2009 to September 2017 (one measurement per day).

2.3. Wind Turbines

In Table 2, the main characteristics of the offshore wind turbines considered in the present work are presented, which are currently considered for implementation in European offshore wind projects [42]. The selected turbines cover a full spectrum of rated capacities, starting from 3 MW for the V90-3.0MW system and ending with a 9.5 MW for the V164-9.5MW generator, which is expected to be implemented in near-future projects. The power curves of each device can be identified throughout the cut-in, rated speed and cut-out thresholds, while the hub height was considered the lowest value indicated by the manufacturer, for which the performance of each system was assessed.

Table 2. Technical specifications for the technologies considered.

Turbine	Rated Power (MW)	Cut-in Speed (m/s)	Rated Speed (m/s)	Cut-out Speed (m/s)	Hub Height (m)	Reference
V90-3.0 MW	3	4	15	25	80–105	[43]
Areva M5000-116	5	4	12.5	25	90	[44]
Servion 6.2M126	6.15	3.5	13.5	30	85–95	[45]
V164-8.8 MW	8.8	4	13	25	105–140	[46]
V164-9.5 MW	9.5	3.5	14	25	105–140	[47]

Usually, standard wind datasets are provided for a 10 m height, but, to adjust these values to the hub height of a particular wind turbine, it is possible to use a logarithmic law [48]. In the present work, the wind resources were assessed at 80 m height, which represents the hub height of the V90-3.0 MW system. This logarithmic law is expressed as:

$$U_{80} = U_{10} \frac{\ln(z_{80}) - \ln(z_{10})}{\ln(z_{10}) - \ln(z_0)} \quad (1)$$

where U_{80} represents the wind speed at 80 m, U_{10} is the initial wind speed (at 10 m), z_0 represents the roughness of the sea surface (0.01 m), and z_{10} and z_{80} are the reference heights.

To estimate the Annual Electricity Production (AEP) of a wind turbine, several approaches are available [49]. For the present work, a similar method to that used by Hrafnkelsson et al. [50] and Salvação and Guedes Soares [51] was used. It can be defined as:

$$AEP = T \times \int_{cut-in}^{cut-out} f(u)P(u)du \quad (2)$$

where AEP is expressed in MWh, T represents the average hours per year (8760 h/year), $f(u)$ is the Weibull probability density function, $P(u)$ is the power curve of a turbine, and cut-in and cut-out represent the turbine characteristics presented in Table 2. Figure 2 illustrates the U_{80} histogram of four sites and the turbine power curves. From the combination of the wind histograms and power curves, we can easily notice that better performances may be expected for Sites P1 and P9, which present a more consistent presence of the wind conditions higher than 10 m/s.

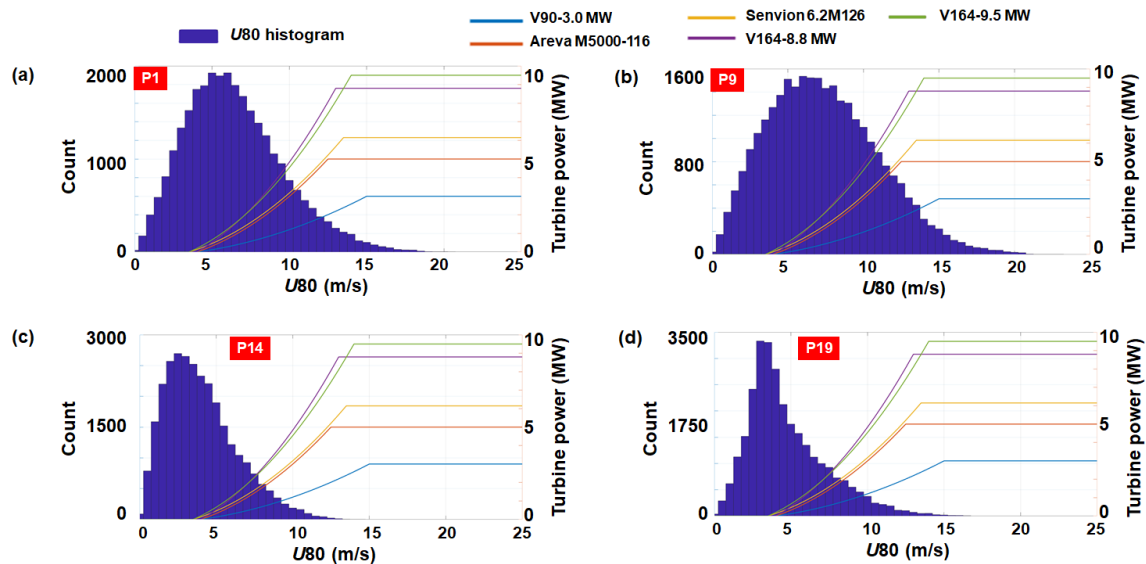


Figure 2. Representation of the wind turbine power curves and wind speed histograms (U_{80}). The wind distribution is related to the ERA-Interim project (January 1998–December 2017) and includes the sites: (a) P1; (b) P9; (c) P14; and (d) P19.

3. Results

3.1. Analysis of the Wind Data

A first analysis is presented in Figure 3, where a direct comparison between the AVISO measurements and the ERA-Interim data was carried out. Figure 3a presents the percentage of the missing values corresponding to the satellite data for each site, from which we can notice three categories. The first one is related to 100% missing values (no data) which include sites such as P1, P13 and P19. This indicates that for these sites another type of data should be considered. Other sites exceed the 10% limit, which is usually considered acceptable for the accuracy of a dataset [52]. This means that the results are biased for these sites. In the group located below 10%, we may find P5–P11, P16 and P18, while Sites P6–P8 do not exceed 0.35% compared to P9 where a value of 10.5% is reported. Figure 3b illustrates the differences between the two datasets in terms of the 50th and 95th percentiles, where the negative values indicate that the AVISO measurements exceed the ERA-Interim values. In general, it seems that the reanalysis data overestimate the wind resources, which for Sites P5–P10 indicate a maximum difference of 2.9 m/s (95th percentile), while, for Sites P11 (east) and P16 (south), it is possible to notice negative values, which reach a value of 2.1 m/s.

Figure 4 illustrates the distribution of the average U_{80} parameter, reported for various intervals, such as total time (full time distribution), winter season (December–February), spring season (March–May), summer season (June–August) and autumn season (September–November). Usually, the attractiveness of a site for a wind project is indicated throughout wind classes, denoted C1–C7, with higher classes being considered more promising for renewable projects [53]. As expected, the most energetic season is winter, while summer has much lower values. The energy pattern is visible in the case of Sites P1–P10 which indicates values in the range 6–9 m/s, more promising results being expected for Sites P6 (Sevastopol) and P9 (Kerch–Azov Sea), which during the winter present values

located close to C6 wind class. In addition, Sites P18 and P20 seem to be defined by relevant wind resources, which nevertheless do not exceed the C4 class. Much lower wind conditions are noticed near Sites P11–P17 (south and southeast), indicating average values located in the C1 class, regardless of the time interval considered for assessment.

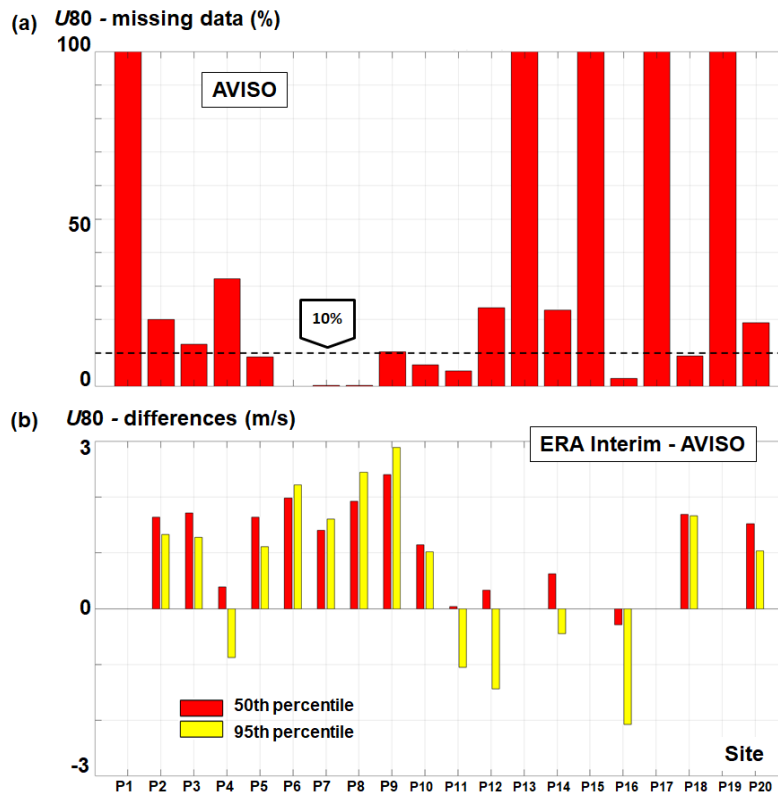


Figure 3. Comparison between the ERA-Interim wind data and the satellite measurements (from AVISO) corresponding to the time interval September 2009–September 2017. Results indicated in terms of: (a) missing data reported by AVISO; and (b) differences reported between ERA-Interim and AVISO data, considering the 50th and 95th percentiles, respectively.

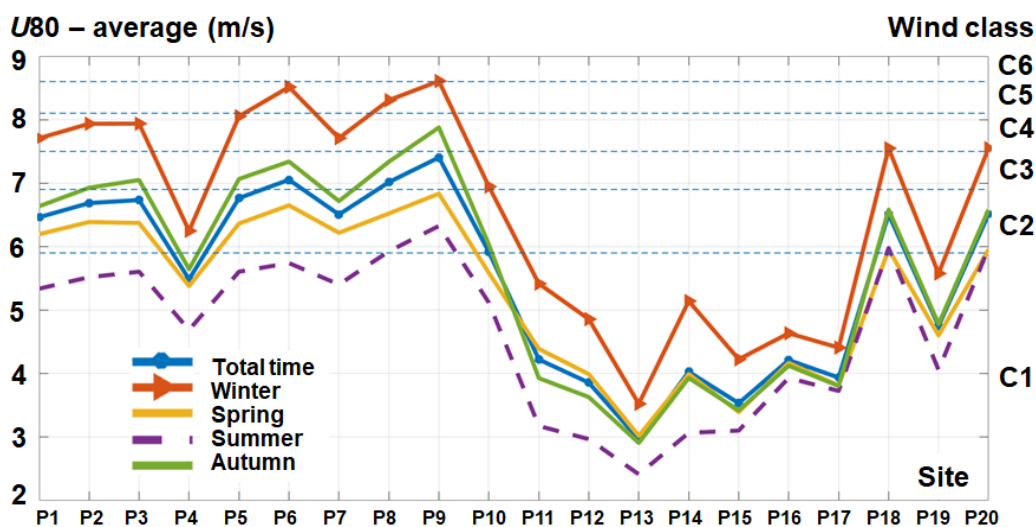


Figure 4. Distribution of the U_{80} average values corresponding to the full time distribution and the representative seasons, considering the ERA-Interim data (January 1998–December 2017). The wind class levels (C1–C6) are also indicated.

In Figure 5, the Weibull distributions are illustrated, considering all the reference sites. These results are based on the ERA-Interim data (total time) and provide some insights regarding the distribution of the wind resources by intervals and the energy potential of a particular site. Much lower performances are expected for Sites P13, P15 and P17 which present peaks around 2–3 m/s.

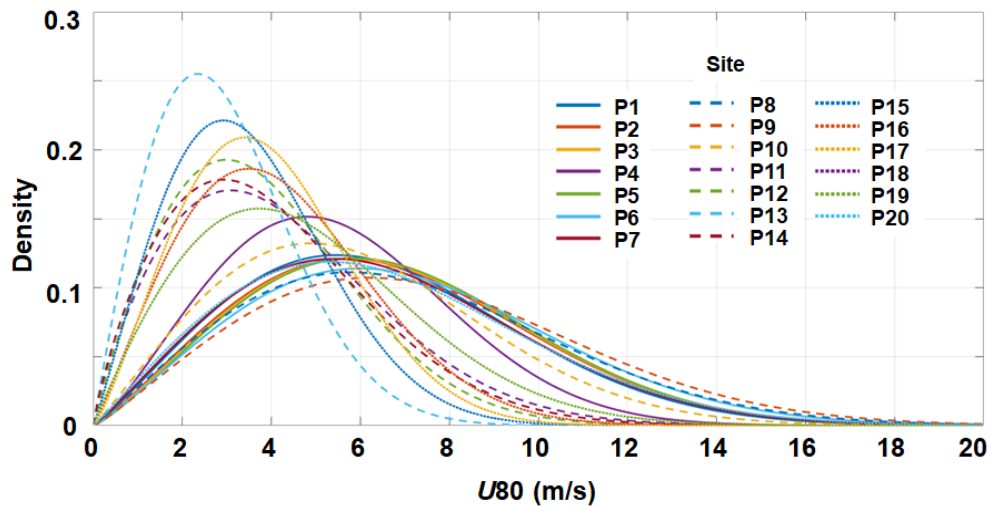


Figure 5. The Weibull distributions corresponding to the ERA-Interim values (January 1998–December 2017).

Another important parameter is the wind direction, which is represented in Figure 6 for Sites P3, P10, P14 and P18 considering only the total time data, distributed by wind classes, from which we can mention that only Site P18 indicates wind conditions coming from the offshore area. Each site has a different pattern indicating for Site P3 a significant distribution from the northern sector, compared to P10 where maximum 8% may be expected from the northeast. Site P18 presents a similar pattern as P10, while in the case of Trabzon site (P14) most of the wind resources are coming from the onshore area, compared to similar ones coming from the sea, which seem to be less energetic.

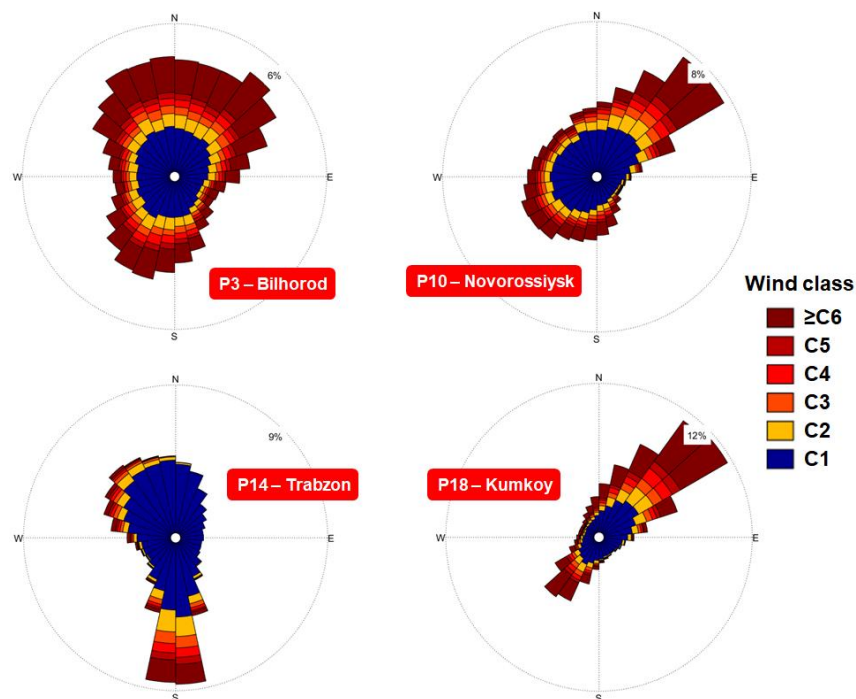


Figure 6. The directional wind distribution, expressed in terms of the wind classes (C1–C6). The full time distribution corresponds to the ERA-Interim data (January 1998–December 2017).

Table 3 summarizes some statistical results presented for each season. Significant variations may occur in the case of the wind direction, as we can see for Sites P13 and P18, which during winter and summer intervals may indicate differences of 56.55° and 62.56° , respectively. In the case of P2, this variation is around 21.39° , which is quite similar to the ones reported between winter and autumn (23.18°). As for the distribution of C3–C6 classes, we may expect that during the winter Sites P2, P9 and P18 reach values in the interval 47–59%, compared to a minimum of 0.9 % reported by P13. These values gradually decrease as we shift to the summer season where a maximum of 34.26% was found at P9, while P13 indicates a value close to zero.

Table 3. U80 seasonal statistics indicated for some of the reference sites. The results are related to the ERA-Interim data and cover the interval from January 1998 to December 2017.

	Winter			Spring			
	U80 (m/s)	Dir (°)	C3–C6 (%)	U80 (m/s)	Dir (°)	C3–C6 (%)	
P2	7.93	189.02	52.64	P2	6.37	172.74	33.99
P9	8.61	169.65	59.00	P9	6.83	168.56	39.55
P13	3.52	183.43	0.88	P13	3.02	206.74	0.42
P18	7.55	160.41	46.99	P18	5.95	143.63	27.39
	Summer			Autumn			
P2	5.52	167.66	21.52	P2	6.93	165.84	39.88
P9	6.32	156.63	34.26	P9	7.88	154.94	50.86
P13	2.41	239.98	0.04	P13	2.91	195.09	0.78
P18	5.98	97.85	29.47	P18	6.58	130.94	36.78

3.2. Evaluation of the Wind Turbine Performance

For the wind turbines, a first indicator considered for assessment is the Capacity Factor (C_f in %), which is frequently used to estimate the efficiency of a turbine. This can be defined as [25]:

$$C_f = \frac{P_{turbine}}{P_{rated}} \cdot 100 \quad (3)$$

where $P_{turbine}$ is the theoretical energy output of a wind turbine (in MW) and P_{rated} is the rated power of a wind turbine (in MW) mentioned in Table 2.

Figure 7 illustrates the distribution of this index, where the values are sorted in descending order. The first places include Sites P9, P8, P6 and P5 (Crimea Peninsula) while on the opposite side we may find P12, P17, P15 and P13. In the case of the Areva M5000-116 system, we may notice better performances, which reach a maximum of 35% at P9, 25.7% at P1 and 2% at P13. The turbines Senvion 6.2M126 and V164-8.8 MW have similar values, which are almost identical as the values decrease through P10 (19.1%). For the sites located on the lower end of this chart, it seems that they have the same efficiency regardless of the rated capacity considered, while turbine V90-3.0 MW presents much lower values. By comparing the values reported by Areva M5000-116 with the ones from V90-3.0 MW, we observe the following differences: P9, 11%; P2 and P1, 8%; P11, 3%; and P13, 0.8%.

Another important index is the rated capacity (in %) which expresses the percentage of the time during which a particular turbine will operate at full capacity, being defined as the wind distribution between the rated speed and the cut-out speed. In Figure 8, we can see the evolution of this parameter, which does not exceed 10% and has a similar distribution as in the case of the C_f index, where the system Areva M500-116 presents the best performances compared to V90-3.0 MW, which is on the last place. In the first places, we find P9, P8 and P6, which report values in the range 7.42–9.8%. The values are gradually decreasing for the reference points P18 (5.4%) and P5 (5.3%), while as we approach to Site P19 there is a decrease of this index below the 1.2% limit. A maximum value of 2.9% is reported by the system V90-3.0 MW close to Site P9, while turbine V164-9.5 MW, which has the highest rated

capacity, presents values in the range 3.85–5.25% for the group Sites P6–P9 and a sharp decrease from 2.5% (Site P5) to 0.5% (Site P19).

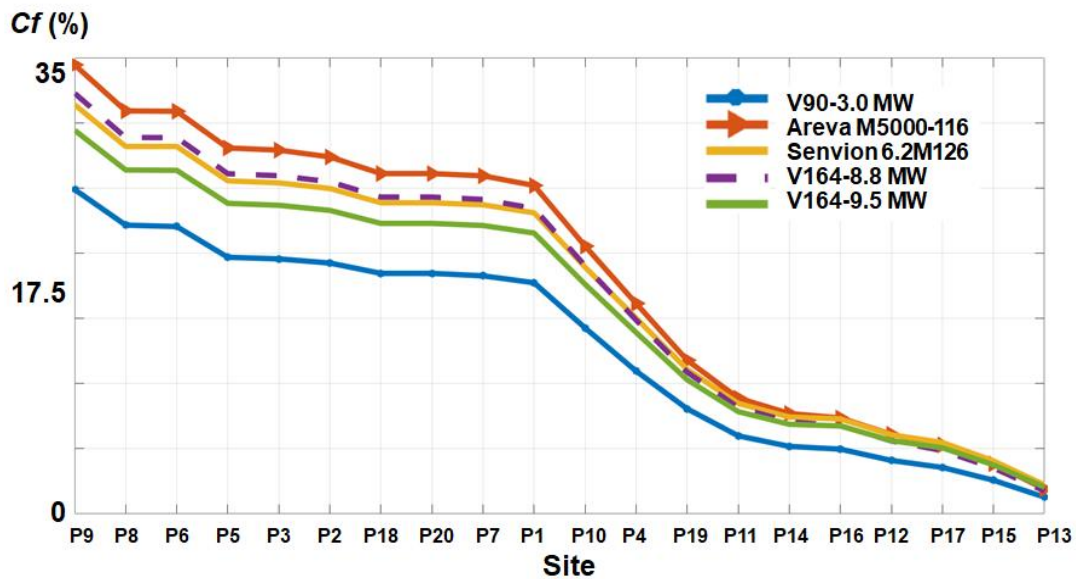


Figure 7. Capacity factor (in %) of the wind turbines considering the ERA-Interim data for the time interval January 1998–December 2017.

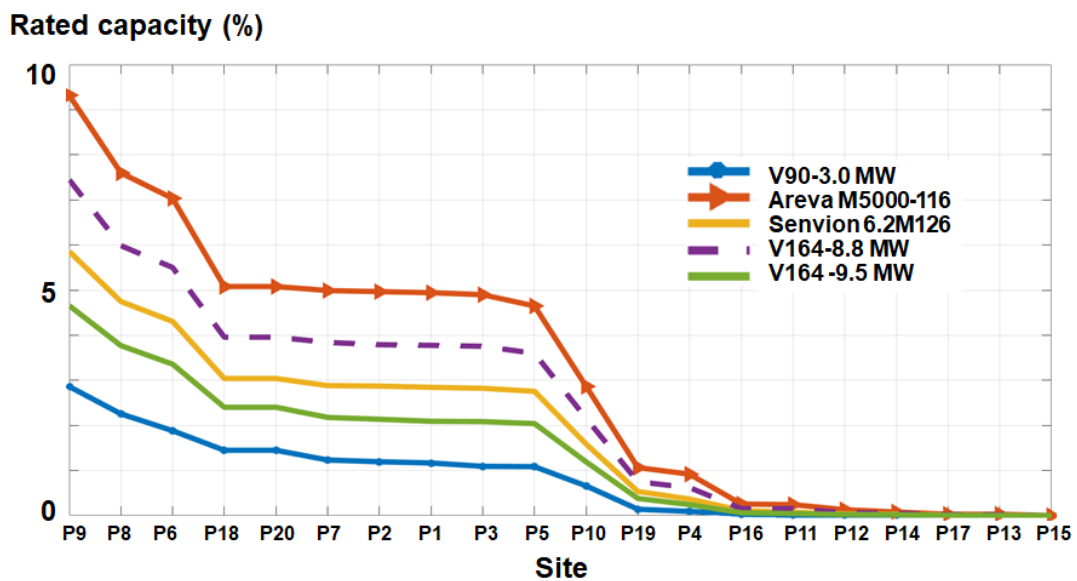


Figure 8. The rated capacity (in %) of the wind turbines which may operate in the Black Sea area. Results based on the ERA-Interim data covering the interval January 1998–December 2017.

Figure 9 presents the evolution of the AEP index, from which we can notice that this is influenced by the local wind resources and by the rated power of the turbine. In this case, better performances are reported by the systems V164-8.8 MW and V164-9.5 MW, which seem to have similar values indicating a maximum of 24,738 MWh near P9 and a minimum of 1747 MWh at P13. From the Areva M5000-116 and Senvion 6.2M126, the second turbine seems to generate more electricity, the differences between them being around: P1, 1319 MWh; P6, 1532 MWh; P11, 620 MWh; P16, 659 MWh; and P20, 1326 MWh. The system V90-3.0MW seems to be the less attractive turbine for the Black Sea environment, presenting much lower AEP values. For the interval P1–P9, this indicates values in the range 4657–6539 MWh,

except the peak of 2876 MWh for Site P4. Sites P11–P17 account for the lowest values, indicating a minimum of 337 MWh (P13) and a maximum of 1573 MWh (P11).

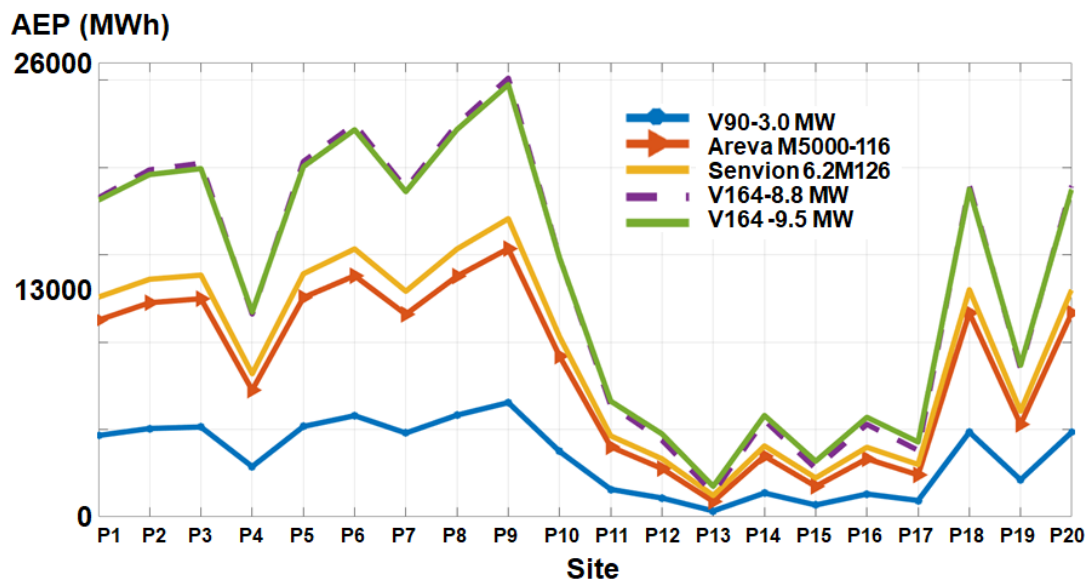


Figure 9. Annual Energy Production (AEP in MWh) of the offshore wind turbines.

Table 4 presents a more detailed assessment of the AEP index, by considering the seasonal fluctuations. As expected, the winter dominates with more impressive values, and at a first look it seems that the differences reported between the systems Areva M5000-116 and Senvion 6.2M126 are more significant than similar ones indicated for the Vestas turbines rated at 8.8 MW and 9.5 MW. In addition, it is important to mention that, in most cases, the system rated at 8.8 MW exceeds the AEP values reported by the 9.5 MW turbine, which indicate that probably for this coastal environment the first turbine will be more suitable. During the summer, we may expect a minimum of 94 MWh in P13, which may easily increase to 726 MWh if a V164-9.5 MW turbine were used.

Table 4. The AEP production (MWh) corresponding to the offshore wind turbines on a seasonal level. Results available for the interval from January 1998 to December 2017 (ERA-Interim wind data).

Turbine	Winter						Spring				
	T1	T2	T3	T4	T5		T1	T2	T3	T4	T5
P2	7325	17,303	19,155	29,187	28,654	P2	4458	11,016	12,188	18,497	18,219
P9	8748	20,042	22,320	33,925	33,431	P9	5561	13,207	14,699	22,274	21,989
P13	593	1537	2053	2622	3129	P13	338	880	1236	1510	1893
P18	6827	15,806	17,637	26,750	26,457	P18	3870	9468	10,608	15,934	15,856
Turbine	Summer						Autumn				
	T1	T2	T3	T4	T5		T1	T2	T3	T4	T5
P2	3033	7575	8544	12,721	12,785	P2	5453	13,229	14,623	22,254	21,866
P9	4468	11,038	12,210	18,507	18,217	P9	7428	17,225	19,180	29,165	28,716
P13	94	254	458	451	726	P13	320	836	1153	1423	1760
P18	3704	9381	10,369	15,672	15457	P18	5025	12,121	13,472	20,414	20,145

T1, V90-3.0 MW; T2, Areva M5000-116; T3, Senvion 6.2M126; T4, V164-8.8 MW; T5, V164-9.5 MW.

4. Discussion

Since there are currently no operational offshore wind projects in the Black Sea area, the purpose of this section is to identify some suitable projects that may be implemented in this region. One way

is to compare the wind resources from the Black Sea sites with the ones reported near some offshore wind farms that are already operating in Europe.

Figure 10 presents the distribution of the U_{80} parameter (average values based on U_{10} satellite measurements) for Sites P1–P20. As noticed, some sites have missing values (*NaN*, Not A Number values) which may indicate that the selected sites are located too close to the coastline and the satellite missions are not able to accurately measure the local wind conditions. Much lower values are reported compared to ERA-Interim data (Figure 4), while in this case the reference location P5 seems to have the best wind resources compared to P9 as indicated by the reanalysis dataset. The sites located in Sector A report relatively small differences, while the sites located in Sector C seem to register moderate wind resources, a minimum of 3.78 m/s being observed close to P14.

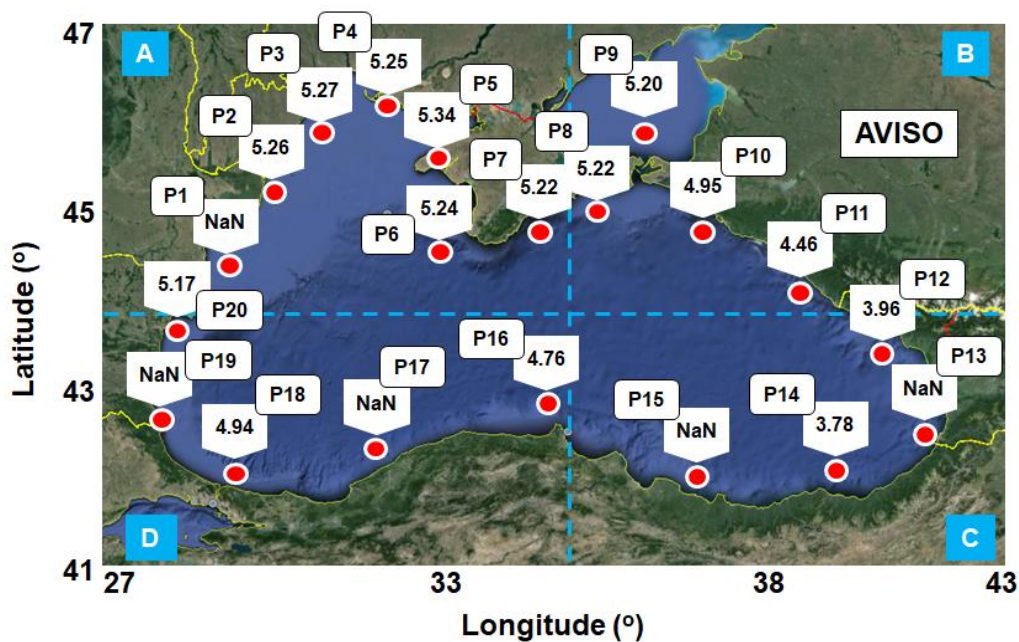


Figure 10. U_{80} average values reported by the AVISO measurements (September 2009–September 2017).

Although the best sites from the point of view of the wind resources seem to be located close to the Crimea Peninsula, considering the current geopolitical issues, it is difficult to believe that a renewable project can be developed in the near future. Therefore, attention probably needs to be shifted to an EU country, such as Romania, which also seems to present better wind resources according to AVISO and ERA-Interim data, thus Site P2 is considered for comparison with some European projects.

The wind conditions in the vicinity of 171 offshore wind projects [42] were considered for assessment, including projects in Belgium, Denmark, France, Germany, Netherlands, Sweden and United Kingdom. By comparing the wind resources at Site P2 (Black Sea, Romania) with the ones in Europe, a top 10 best agreement was identified, as presented in Figure 11. The projects in the early stages of development are denoted with an asterisk symbol (*) and more details about them can be found in Table 5. According to the AVISO values (Figure 11a), all of the European sites seem to have better wind resources than Site P2, on average values are between 5.7 m/s and 5.9 m/s, being noticed a constant distribution between Borkum and Wikinger.

In Figure 11b, we can identify the water depth and the distance from the coastline of the selected sites. From these combinations, it results that Site P2 is located a similar distance from the shore as the Bockstingen and Nenuphar sites, which are used as test sites. As for the water depth, much lower values are reported by two operational projects from Germany (EnBW Baltic1, 48.3 MW; and Borkum Riffgrund 1, 582 MW) and by two early development stage projects from Sweden and Denmark (Kriegers Flak, 590 MW; and Kriegers Flak II, 640 MW).

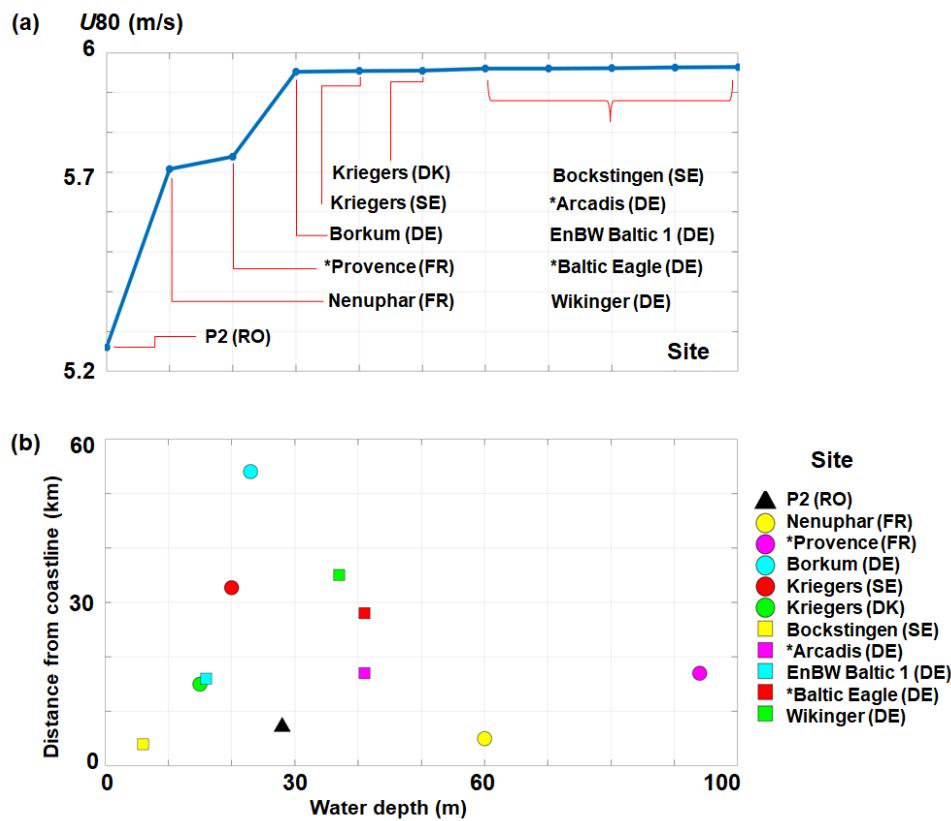


Figure 11. Direct comparison between the wind conditions reported close to reference point P2 and some European wind projects, where the dataset correspond to the AVISO measurements (September 2009–September 2017). The results correspond to: (a) U_{80} comparison; and (b) main characteristics of the selected sites.

Table 5. The European offshore wind projects considered for comparison [42].

No.	Project	Country	Status	Project Capacity (MW)	Turbine Model	Water Depth (m)	Distance from Coastline (km)
1	Nénuphar (test site)	France	Consent authorized	10	Not decided	60–70	5
2	Provence (floating)	France	Early planning	24	SWT-8.0-154	94–104	17
3	Borkum Riffgrund 1	Germany	Operational	582	SWT-6.0-154	28–34	45
4	Kriegers Flak II	Sweden	Consent authorized	640	Not decided	20–40	32.7
5	Kriegers Flak	Denmark	Pre-construction	590	SG 8.0-167 DD	15–30	15
6	Bockstingen	Sweden	Operational	2.75	Wind World 550 kW	6	4
7	Arcadis Ost 1	Germany	Consent authorized	247	Haliade 150-6 MW	41–46	17
8	EnBW Baltic 1	Germany	Operational	48.3	SWT-2.3-93	16–19	16
9	Baltic Eagle	Germany	Consent authorized	476	Not decided	41–44	28
10	Wikinger	Germany	Operational	350	AD 5-135	37–43	35

According to the CIA World Factbook [54], during 2015–2017, the estimated electricity productions of the countries located around the Black Sea were around: Romania, 62.16 billion kWh; Ukraine, 152.2 billion kWh; Russia, 1.008 trillion kWh; Georgia, 11.57 billion kWh; Turkey, 245.8 billion kWh; and Bulgaria, 45.04 billion kWh. To reach at least 1% of this capacity for Romania with offshore wind turbines, according to the AEP values presented in Figure 9, it would be necessary for at least 123 V90-3.0 MW turbines (denoted with T1) or 32 V164-9.5 MW turbines (denoted with T5) (Site P2) to be installed. For the rest of the countries, we may estimate: Ukraine (Site P3), 296 T1 systems or 76 T5 systems; Georgia (P13), 344 T1 systems or 66 T5 systems; Turkey (Site P18), 507 T1 systems or 131 T5 systems; and Bulgaria (Site P20), 93 T1 systems or 24 T5 systems. The most energetic sites were considered for assessment, while the sites from Russia were not included in this analysis since the necessary number of turbines cannot be supported by a single site.

Referring to similar studies focused on the Black Sea wind energy assessment, such as the one presented by Ona and Rusu [25], we can notice that the western part of this region seems to reveal more important wind resources, in particular close to the Romanian nearshore. In that work, the sites are defined for a water depth located close to 50 m, while the evaluation uses a different wind dataset coming from US National Centers for Environmental Prediction, which is processed for 1979–2010. Regarding the performances of a wind turbine, the same work highlights that the Senvion 6.2M126 generator may reveal close to the Crimean Peninsula (northwest) a maximum of 7.3%, which is much higher than the one reported in this work. Nevertheless, compared to some other previous works, which are focused on the assessment of various wind turbines performances [48,55], the present approach seems to be more exact. This is because it involved the combination of a Weibull probability density function and the power curve of the turbine, while some previous works use a method that considers various values of the Betz coefficient, sometimes chosen close to the ideal threshold (59%), which cannot be considered realistic for a wind project.

5. Conclusions

In the present work, the nearshore wind energy resources from the Black Sea region were assessed by considering some environmental parameters (such as U_{80}) and the power curves of some state-of-the-art wind turbines, which operate or are currently implemented in European offshore wind projects. Based on the ERA-Interim reanalysis dataset (corresponding to 1998–2017) and AVISO satellite measurements (corresponding to September 2009–September 2017), it was possible to highlight the dominant energy patterns from this area, revealing some hot-spots, which can be used for developing future wind projects. Both wind datasets indicate the Crimea Peninsula region as being one of the most energetic regions in the Black Sea. While ERA-Interim indicates the sites from the Azov Sea as being more important, AVISO highlights the sites from the western coast of this peninsula. Since there are currently no nearshore or offshore wind projects in this region, another direction of the present work was related to the assessment of the performances provided by some standard wind turbines and to estimate what kind of projects could operate in this region. According to these results, it seems that the Black Sea may be suitable for the development of wind projects, especially in the western part of the basin which is dominated by a lower water depth, in particular for the development of some pilot projects or test sites.

The main findings of this work are:

1. From the literature review, it was highlighted the fact that wind resources in the Black Sea are not very often evaluated from the point of view of a renewable energy project, most of the research being focused on climatological studies or calibrations of the numerical models.
2. The Crimea Peninsula seems to present the most attractive wind resources, but considering the current geopolitical situation, the likelihood of a wind project in the near future in those coastal waters is not high.
3. Considering the expected performances of the V90-3.0 MW, we can say that this is not a viable candidate for the Black Sea area. A lower rated wind speed system, such as Areva M5000-116, seems to be more efficient for this coastal environment.
4. A wind project, including high capacity turbines, seems to be more productive in the western and northern parts of the Black Sea (Sectors A and B). There is a significant difference between the results reported by Senvion 6.2M126 and V164-8.8 MW or V164-9.5 MW, while for latter two turbines the results are almost identical in the case of the AEP index. For most sites, better results are reported by the system rated at 8.8 MW.
5. Based on the electricity production statistics and the computed AEP values, it was possible to estimate the required number of turbines to reach at least 1% of the national share. The results indicate that, for the western part of the Black Sea, this target can be easily achieved throughout one or two wind farms projects.

Author Contributions: F.O. performed the literature review, processed the wind data, carried out the statistical analysis and interpreted the results. L.R. guided this research, wrote the final form of the manuscript and drew the conclusions. The final manuscript was approved by all authors.

Funding: This work was supported by a grant of Ministry of Research and Innovation, CNCS—UEFISCDI, project number PN-III-P1-1.1-PD-2016-0235, within PNCDI III.

Acknowledgments: ECMWF ERA-Interim data used in this study were obtained from the ECMWF data server. The altimeter products were generated and distributed by Aviso (<http://www.aviso.altimetry.fr/>) as part of the SSALTO ground processing segment.

Conflicts of Interest: The authors declare no conflict of interest.

Nomenclature

ACCWA	Assessment of the Climate Change effects on the WAve conditions in the Black Sea
AEP	Annual Electricity Production
AVISO	Archiving, Validation and Interpretation of Satellite Oceanographic Data
DAMWAVE	Data Assimilation Methods for improving the WAVE predictions in the Romanian nearshore of the Black Sea
ECMWF	European Centre for Medium-Range Weather Forecasts
NaN	Not A Number
C _f	capacity factor
T	average hours per year (8760 h/year)
U ₁₀	wind speed reported at 10 m above sea level
U ₈₀	wind speed reported at 80 m above sea level
z ₀	roughness of the sea surface (0.01 m)
P(u)	power curve of a turbine
f(u)	Weibull probability density function
z ₁₀ ; z ₈₀	reference heights

References

- Ji, Q.; Zhang, D.; Geng, J. Information linkage, dynamic spillovers in prices and volatility between the carbon and energy markets. *J. Clean. Prod.* **2018**, *198*, 972–978. [[CrossRef](#)]
- Wang, Y.; Guo, Z. The dynamic spillover between carbon and energy markets: New evidence. *Energy* **2018**, *149*, 24–33. [[CrossRef](#)]
- Child, M.; Koskinen, O.; Linnanen, L.; Breyer, C. Sustainability guardrails for energy scenarios of the global energy transition. *Renew. Sustain. Energy Rev.* **2018**, *91*, 321–334. [[CrossRef](#)]
- Armeanu, D.Ş.; Vintilă, G.; Gherghina, Ş.C. Does Renewable Energy Drive Sustainable Economic Growth? Multivariate Panel Data Evidence for EU-28 Countries. *Energies* **2017**, *10*, 381. [[CrossRef](#)]
- Karakosta, C. A holistic approach for addressing the issue of effective technology transfer in the frame of climate change. *Energies* **2016**, *9*, 503. [[CrossRef](#)]
- Castro-Santos, L.; Martins, E.; Guedes Soares, C. Methodology to calculate the costs of a floating offshore renewable energy farm. *Energies* **2016**, *9*, 324. [[CrossRef](#)]
- Willis, D.J.; Niezrecki, C.; Kuchma, D.; Hines, E.; Arwade, S.R.; Barthelmie, R.J.; DiPaola, M.; Drane, P.J.; Hansen, C.J.; Inalpolat, M. Wind energy research: State-of-the-art and future research directions. *Renew. Energy* **2018**, *125*, 133–154. [[CrossRef](#)]
- Poulsen, T.; Hasager, C.B. The Revolution of China: Offshore Wind Diffusion. *Energies* **2017**, *10*, 2153. [[CrossRef](#)]
- Lapworth, A. The diurnal variation of the marine surface wind in an offshore flow. *Q. J. R. Meteorol. Soc.* **2005**, *131*, 2367–2387. [[CrossRef](#)]
- Global Statistics. Available online: <http://gwec.net/global-figures/graphs/> (accessed on 15 August 2018).
- The European Offshore Wind Industry—Key Trends and Statistics 2017. Available online: <https://windeurope.org/about-wind/statistics/offshore/european-offshore-wind-industry-key-trends-statistics-2017/> (accessed on 15 August 2018).

12. Rusu, E.; Onea, F. Joint Evaluation of the Wave and Offshore Wind Energy Resources in the Developing Countries. *Energies* **2017**, *10*, 1866. [[CrossRef](#)]
13. Rusu, L.; Onea, F. The performance of some state-of-the-art wave energy converters in locations with the worldwide highest wave power. *Renew. Sustain. Energy Rev.* **2017**, *75*, 1348–1362. [[CrossRef](#)]
14. Rusu, L.; Bernardino, M.; Guedes Soares, C. Wind and wave modelling in the Black Sea. *J. Oper. Oceanogr.* **2014**, *7*, 5–20. [[CrossRef](#)]
15. Rusu, L.; Ganea, D.; Mereuta, E. A joint evaluation of wave and wind energy resources in the Black Sea based on 20-year hindcast information. *Energy Explor. Exploit.* **2018**, *36*, 335–351. [[CrossRef](#)]
16. Valchev, N.N.; Trifonova, E.V.; Andreeva, N.K. Past and recent trends in the western black sea storminess. *Nat. Hazards Earth Syst. Sci.* **2012**, *12*, 961–977. [[CrossRef](#)]
17. Onea, F.; Rusu, E. Wind energy assessments along the Black Sea basin. *Meteorol. Appl.* **2014**, *21*, 316–329. [[CrossRef](#)]
18. Akpınar, A.; Ponce de León, S. An assessment of the wind re-analyses in the modelling of an extreme sea state in the black sea. *Dyn. Atmos. Ocean.* **2016**, *73*, 61–75. [[CrossRef](#)]
19. Koletsis, I.; Kotroni, V.; Lagouvardos, K.; Soukissian, T. Assessment of offshore wind speed and power potential over the mediterranean and the black seas under future climate changes. *Renew. Sustain. Energy Rev.* **2016**, *60*, 234–245. [[CrossRef](#)]
20. Damwave. Available online: http://www.im.ugal.ro/DAMWAVE/index_engleza.htm (accessed on 25 March 2018).
21. ACCWA. Available online: http://193.231.148.42/accwa/index_en.php# (accessed on 25 March 2018).
22. Davy, R.; Gnatiuk, N.; Pettersson, L.; Bobylev, L. Climate change impacts on wind energy potential in the European domain with a focus on the Black Sea. *Renew. Sustain. Energy Rev.* **2018**, *81*, 1652–1659. [[CrossRef](#)]
23. Onea, F.; Rusu, E. An Evaluation of the Wind Energy in the North-West of the Black Sea. *Int. J. Green Energy* **2014**, *11*, 465–487. [[CrossRef](#)]
24. İlkiliç, C.; Aydin, H. Wind power potential and usage in the coastal regions of turkey. *Renew. Sustain. Energy Rev.* **2015**, *44*, 78–86. [[CrossRef](#)]
25. Onea, F.; Rusu, E. Efficiency assessments for some state of the art wind turbines in the coastal environments of the black and the caspian seas. *Energy Explor. Exploit.* **2016**, *34*, 217–234. [[CrossRef](#)]
26. Arğin, M.; Yerci, V. The assessment of offshore wind power potential of Turkey. In Proceedings of the 2015 9th International Conference on Electrical and Electronics Engineering (ELECO), Bursa, Turkey, 26–28 November 2015; pp. 966–970.
27. Raileanu, A.B.; Onea, F.; Rusu, E. Evaluation of the Offshore Wind Resources in the European Seas Based on Satellite Measurements. In Proceedings of the Conference: International Multidisciplinary Scientific GeoConferences SGEM, Albena, Bulgaria, 16–25 June 2015; pp. 227–234.
28. Arkhipkin, V.S.; Gippius, F.N.; Koltermann, K.P.; Surkova, G.V. Wind waves in the Black Sea: Results of a hindcast study. *Nat. Hazards Earth Syst. Sci.* **2014**, *14*, 2883–2897. [[CrossRef](#)]
29. Kosarev, A.N. *The Black Sea Environment*; Springer-Verlag: Berlin, Germany, 2008; pp. 11–30, ISBN 978-3-540-74291-3.
30. ERA-Interim. Available online: <https://www.ecmwf.int/en/forecasts/datasets/archive-datasets/reanalysis-datasets/era-interim> (accessed on 18 August 2018).
31. Dee, D.P.; Uppala, S.M.; Simmons, A.J.; Berrisford, P.; Poli, P.; Kobayashi, S.; Andrae, U.; Balsameda, M.A.; Balsamo, G.; Bauer, P. The ERA-Interim reanalysis: Configuration and performance of the data assimilation system. *Q. J. R. Meteorol. Soc.* **2011**, *137*, 553–597. [[CrossRef](#)]
32. Zheng, C.; Xiao, Z.; Peng, Y.; Li, C.; Du, Z. Rezoning global offshore wind energy resources. *Renew. Energy* **2018**, *129*, 1–11. [[CrossRef](#)]
33. Dupont, E.; Koppelaar, R.; Jeanmart, H. Global available wind energy with physical and energy return on investment constraints. *Appl. Energy* **2018**, *209*, 322–338. [[CrossRef](#)]
34. Onea, F.; Rusu, E. Sustainability of the Reanalysis Databases in Predicting the Wind and Wave Power along the European Coasts. *Sustainability* **2018**, *10*, 193. [[CrossRef](#)]
35. Carvalho, D.; Rocha, A.; Gómez-Gesteira, M.; Silva Santos, C. Offshore wind energy resource simulation forced by different reanalyses: Comparison with observed data in the iberian peninsula. *Appl. Energy* **2014**, *134*, 57–64. [[CrossRef](#)]

36. Gallagher, S.; Tiron, R.; Whelan, E.; Gleeson, E.; Dias, F.; McGrath, R. The nearshore wind and wave energy potential of Ireland: A high resolution assessment of availability and accessibility. *Renew. Energy* **2016**, *88*, 494–516. [CrossRef]
37. Wan, Y.; Fan, C.; Dai, Y.; Li, L.; Sun, W.; Zhou, P.; Qu, X. Assessment of the Joint Development Potential of Wave and Wind Energy in the South China Sea. *Energies* **2018**, *11*, 398. [CrossRef]
38. Kim, H.-G.; Kim, J.-Y.; Kang, Y.-H. Comparative Evaluation of the Third-Generation Reanalysis Data for Wind Resource Assessment of the Southwestern Offshore in South Korea. *Atmosphere* **2018**, *9*, 73. [CrossRef]
39. Mattar, C.; Borvarán, D. Offshore wind power simulation by using WRF in the central coast of Chile. *Renew. Energy* **2016**, *94*, 22–31. [CrossRef]
40. MSWH/MWind: Aviso+. Available online: <https://www.aviso.altimetry.fr/en/data/products/windwave-products/mswhmwind.html> (accessed on 18 August 2018).
41. Pujol, M.-I.; Faugère, Y.; Taburet, G.; Dupuy, S.; Pelloquin, C.; Ablain, M.; Picot, N. DUACS DT2014: The new multi-mission altimeter data set reprocessed over. *Ocean Sci.* **2016**, *12*, 1067–1090. [CrossRef]
42. Global Offshore Wind Farms Database–4C Offshore. Available online: <https://www.4coffshore.com/windfarms/> (accessed on 19 May 2018).
43. Vestas V90-3.0-300 MW-Wind Turbine. Available online: <https://en.wind-turbine-models.com/turbines/603-vestas-v90-3.0> (accessed on 29 July 2018).
44. AREVA M5000-116-500 MW-Wind Turbine. Available online: <https://en.wind-turbine-models.com/turbines/23-areva-m5000-116> (accessed on 29 July 2018).
45. 6.2M126-Wind Turbine 6.2 MW. Available online: <https://www.senvion.com/global/en/products-services/wind-turbines/6xm/62m126/> (accessed on 19 August 2018).
46. MHI Vestas Offshore V164-8.8 MW-880 MW-Wind Turbine. Available online: <https://en.wind-turbine-models.com/turbines/1819-mhi-vestas-offshore-v164-8.8-mw> (accessed on 19 August 2018).
47. MHI Vestas Offshore V164/9500–Manufacturers and turbines–Online Access–The Wind Power. Available online: https://www.thewindpower.net/turbine_en_1476_mhi-vestas-offshore_v164-9500.php (accessed on 19 August 2018).
48. Onea, F.; Deleanu, L.; Rusu, L.; Georgescu, C. Evaluation of the wind energy potential along the Mediterranean Sea coasts. *Energy Explor. Exploit.* **2016**, *34*, 766–792. [CrossRef]
49. Manwell, J.F.; McGowan, J.G.; Rogers, A.L. Wind Energy Explained: Theory, design and application. *Wind Eng.* **2006**, *30*, 169–170. [CrossRef]
50. Carballo, R.; Iglesias, G. A methodology to determine the power performance of wave energy converters at a particular coastal location. *Energy Convers. Manag.* **2012**, *61*, 8–18. [CrossRef]
51. Salvacao, N.; Guedes Soares, C. Wind resource assessment offshore the Atlantic Iberian coast with the WRF model. *Energy* **2018**, *145*, 276–287. [CrossRef]
52. Dong, Y.; Peng, C.-Y.J. Principled missing data methods for researchers. *SpringerPlus* **2013**, *2*, 222. [CrossRef] [PubMed]
53. Archer, C.L.; Jacobson, M.Z. Spatial and temporal distributions of US winds and wind power at 80 m derived from measurements. *J. Geophys. Res.* **2003**, *108*, 4289. [CrossRef]
54. The World Factbook. Available online: <https://www.cia.gov/library/publications/the-world-factbook/> (accessed on 15 Jun 2018).
55. Onea, F.; Rusu, E. The expected efficiency and coastal impact of a hybrid energy farm operating in the Portuguese nearshore. *Energy* **2016**, *97*, 411–423. [CrossRef]

